IOWA STATE UNIVERSITY
Digital Repository

Materials Science and Engineering Publications | Materials Science and Engineering

1-25-2017

Microstructure and oxidation behavior of Al + Cr co-deposited coatings on nickel-based superalloys

R. Q. Lin
Shanghai Key Laboratory of Advanced Ferrometallurgy

C. Fu
Shanghai Electric Group Co., Ltd.

M. Liu
Shanghai Key Laboratory of Advanced Ferrometallurgy

H. Jiang
Shanghai Key Laboratory of Advanced Ferrometallurgy

X. Li
Shanghai Key Laboratory of Advanced Ferrometallurgy

See next page for additional authors

Follow this and additional works at: https://lib.dr.iastate.edu/mse_pubs

 Part of the Metallurgy Commons

The complete bibliographic information for this item can be found at https://lib.dr.iastate.edu/mse_pubs/315. For information on how to cite this item, please visit http://lib.dr.iastate.edu/howtocite.html.

This Article is brought to you for free and open access by the Materials Science and Engineering at Iowa State University Digital Repository. It has been accepted for inclusion in Materials Science and Engineering Publications by an authorized administrator of Iowa State University Digital Repository. For more information, please contact digirep@iastate.edu.

Microstructure and oxidation behavior of Al + Cr co-deposited coatings on nickel-based superalloys

Abstract
The microstructure and oxidation behavior were investigated in Al and Cr co-deposited diffusion coatings prepared by the pack cementation process. The composition (in wt.%) of the packs was 3NH4Cl-xAl-(25-x)Cr-72Al2O3 with different Al levels (x = 0.5, 1.2, 4, and 10). After the heat-treatment process, the corresponding microstructure of the coatings was Cr + Cr2Ni3 + Al-rich phase, Cr + Cr2Ni3, Cr + NiAl + Ni3Al and NiAl + AlCr2, respectively. The isothermal oxidation tests were performed at 950 °C for up to 100 h in air, and the oxidation kinetic curves were obtained. It indicated that the coatings formed in the packs containing 1.2 wt.% Al had the lowest weight gain, while the weight gain of the coating formed in the packs having 4 wt.% Al was the largest. The presence of Cr in Al and Cr co-deposited coatings promotes Al2O3 generation. The formation mechanisms of Al + Cr co-deposited coatings and the effect of Cr in different types of coatings during the oxidation process were discussed.

Keywords
Coatings, Microstructure, Oxidation, Superalloys, Cr

Disciplines
Materials Science and Engineering | Metallurgy

Comments
This is a manuscript of an article published as Lin, R. Q., C. Fu, M. Liu, H. Jiang, X. Li, Z. M. Ren, A. M. Russell, and G. H. Cao. "Microstructure and oxidation behavior of Al+ Cr co-deposited coatings on nickel-based superalloys." *Surface and Coatings Technology* 310 (2017): 273-277. DOI: 10.1016/j.surfcoat.2016.12.096. Posted with permission.

Creative Commons License

This work is licensed under a Creative Commons Attribution-Noncommercial-No Derivative Works 4.0 License.

Authors
R. Q. Lin, C. Fu, M. Liu, H. Jiang, X. Li, Z. M. Ren, Alan M. Russell, and G. H. Cao

This article is available at Iowa State University Digital Repository: https://lib.dr.iastate.edu/mse_pubs/315

Microstructure and oxidation behavior of Al + Cr co-deposited coatings on nickel-based superalloys

R.Q. Lin[1], C. Fu[1], A.M. Russell[2], G.H. Cao[1]*

[1]*Department of Materials Engineering, Shanghai University, 149 Yanchang Road, Shanghai 200072, China*

[2] *Department of Materials Science and Engineering, Iowa State University and Division of Materials Science and Engineering, Ames Laboratory of the U.S.D.O.E., Ames, IA 50011-2300, USA*

Highlights

1. Co-deposition coatings were prepared by a one-step pack cementation process.
2. The single chromized coatings had good oxidation resistance at 950℃.
3. Higher Cr contents in the coatings stimulate the formation of Al_2O_3.

Abstract

This study investigated the microstructure and oxidation behavior of Al and Cr co-deposited diffusion coatings prepared by the pack cementation process. The composition (in wt.%) of the packs was $3NH_4Cl$-xAl-(25-x)Cr-$72Al_2O_3$ with different Al levels (x = 0.5, 1.2, 4, and 10). After the heat-treatment process, the corresponding microstructure of the coatings was Cr + Cr_2Ni_3 + Al-rich phase, Cr + Cr_2Ni_3, Cr + NiAl + Ni_3Al and NiAl + $AlCr_2$, respectively. The isothermal oxidation tests were performed at 950℃ for up to 100 h in air, and the oxidation kinetic curves were obtained. It indicated that the coatings formed in the packs containing 1.2 wt.% Al had the lowest weight gain, while the weight gain of the coating formed in the packs having 4 wt.% Al was the largest. The presence of Cr in Al and Cr co-deposited coatings promotes Al_2O_3 generation. The formation mechanisms of Al + Cr co-deposited coatings and the effect of Cr in different types of coatings during the oxidation process were discussed.

Keywords: Thermal barrier coatings; Cr; NiAl; Oxidation; Superalloys

1. Introduction

Nickel-based superalloys are unusual metallic materials with excellent physical and mechanical properties. They are widely used in the more severe environments of the aircraft turbine engines, rocket engines, nuclear power and chemical processing plants [1]. Currently, thermal barrier coatings (TBCs) and cooling schemes are used together to reduce the surface temperature of the superalloys; this extends the service life of alloy components in the hottest sections of engines [2-4]. The TBC systems are

* Corresponding author. E-mail address: ghcao@shu.edu.cn (G.H. Cao)

typically two-layer structures, consisting of a ceramic top coat and an underlying metallic bond coat. In order to improve oxidation resistance, the bond coat is sufficiently rich in aluminum to form a protective, thermally grown oxide (TGO) scale of α-Al_2O_3 [3, 4]. The ability to form TGO scale depends on the control of bond-coat composition, microstructure, and surface at all stages of the TGO-formation process [3]. The pack cementation is a representative technique and widely used in diffusion coatings on Ni-based superalloys [5, 6]. Compared to other techniques for the preparation of coatings, pack cementation has the advantages that multiple elements can be deposited simultaneously, and its cost is relatively low.

As a thermochemical diffusion treatment, chromising has undergone several modifications in recent years that have enhanced the process. Powder metallurgy, co-diffusion coatings and new chromising techniques are the three most noteworthy directions of development in the field of chromising [7]. Rastegari et al. [8] and Ledoux et al. [9] have studied the Cr-modified aluminide coating prepared by two-step pack cementation on superalloys. The two-step pack cementation procedure is first pack chromized and then pack aluminized. However, a one-step process is considered to be more economic and convenient. The success of this co-deposition method has been reported in several case studies for iron-based materials [10-12] and TiAl alloys [13, 14]. For the steel substrate, both Al and Cr can diffuse into the substrate to stabilize the ferritic phase. Zheng et al. [11] studied the preparation of $(Fe, Cr)_3Al$ coatings and the properties of oxidation and corrosion resistance. For the Cr-modified aluminide coating on TiAl alloys, the formation of the $Al_{67}Ti_{25}Cr_8$ phase improves stability during cyclic oxidation [15]. The high Cr content TiAl-Cr alloy also promotes dense and compact Al_2O_3 and TiO_2 oxide scales [16].

Recently, the co-deposition of Al and Cr by pack cementation has been found to be effective in Ni-based alloy substrates. Xiang et al. [6] reported that the Al content should be within the range 1.25–1.90 wt.% for the packs activated by 3 wt.% NH_4Cl; the co-diffusion experiments of Al and Cr were carried out with 1.25 wt.%. Al content. For more in-depth study of the formation mechanism of the coatings, coating experiments need to be performed over a range of compositions. In some papers [5, 17-18], the equilibrium vapor pressure of different chloride salt activators were calculated for packs containing Al and Cr. The Cr-modified aluminide coating with oxygen active elements, such as Hf [19], enhanced their corrosion resistance. The hot-corrosion resistance was also influenced by the addition of different Cr content in aluminide coating [20]. By combining thermochemical analysis with experimentation and corrosion resistance research, it was found that co-deposition of Al and Cr could indeed be achieved. Cr_2O_3 and Al_2O_3 are regarded as the best protective oxides because of the relatively slow diffusion in these materials compared to other oxides. However, few investigations have been reported so far of oxidation resistance of the Al and Cr co-deposited coatings on Ni-based superalloys.

Therefore, based on thermochemical analysis of Xiang et al. [6], this study prepared four typical Al and Cr co-deposited coatings with the one-step pack cementation process, and the oxidation behavior of these coatings was investigated. This study focused on the microstructure and formation process of coatings when the

packs have different Al contents. The effects of Cr on co-deposited coatings were also discussed.

2. Experimental procedures

The substrate used for this study is the Ni-based superalloy DZ417G with nominal composition (at.%) of Ni-5.2Al-9.0Cr-10.0Co-4.4Ti-3.0Mo-0.19C-0.7V. The alloys were cut into 3 × 6 × 10mm samples, grit blasted with progressively finer (80 to 2000 mesh) abrasive particles, and ultrasonically cleaned in alcohol. The samples were then exposed to an Al plus Cr pack cementation process. The pack powder mixtures were prepared using Al and Cr as deposition elements, NH_4Cl salt as an activator and Al_2O_3 powder as an inert filler. The composition series was $3NH_4Cl$-xAl-(25-x)Cr-$72Al_2O_3$ (in wt.%) with varying Al content (x = 0.5, 1.2, 1.5, 4, 6, 8, 10 and 12). According to the results, four representative coating samples were selected for further study, as shown in Table 1. The process of pack cementation was performed at 1100℃ for 8 h. To homogenize the microstructure of the coatings, heat-treatments were carried out at 1000℃ in a vacuum quartz tube for 6 h followed by furnace cooling to room temperature.

The oxidation tests were conducted at 950℃ in the range of 5-100 h using a muffle furnace in air. Mass gain of the coatings was measured using an analytical balance every 5 h in the first 20 hours, and every 20 h in the remaining 80 hours. The surface phase constitutions of the coatings and oxides were analyzed with a D/MAX-3C X-ray diffractometer (XRD) with Cu $K_{\alpha 1}$ radiation (λ = 0.1541 nm) in the range 2θ = 20-100° with a step size of 0.02° and a counting time of 1 s per step. The surface morphologies of the oxides and the cross-sectional micrographs of the coatings were examined by an S-3400N scanning electron microscope (SEM) equipped with energy-dispersive X-ray (EDX) spectroscopy. The micro-region X-ray diffractograms were obtained by a D/MAX-2550 X-ray diffractometer to analyze the phase distributions in cross-section of the coatings.

Table 1 The coatings prepared with varying Al contents in the pack.

Coating no.	Pack composition (wt.%)
#1	$3NH_4Cl$-0.5Al-24.5Cr-$72Al_2O_3$
#2	$3NH_4Cl$-1.2Al-23.8Cr-$72Al_2O_3$
#3	$3NH_4Cl$-4Al-21Cr-$72Al_2O_3$
#4	$3NH_4Cl$-10Al-15Cr-$72Al_2O_3$

3. Results

3.1 Microstructure of the coatings

Fig. 1a shows the X-ray diffraction patterns of coatings #1, #2, #3, and #4 indicating the major phases in the coating surfaces. SEM cross-sectional images of the corresponding four coatings are shown in Figs. 2b-e. The coatings with an Al content of 0.5 wt.% and 1.2 wt.% are chromized coatings. It can be seen that the major phases in coating #1 were Cr and Cr_2Ni_3 with a thickness of 30 μm. A small amount of Al-rich phase (point 1) also existed in the coating. Some acicular Ti-rich phase (point 2) was present in coating #1 in Fig. 1b. Coating #2 consisted of two distinctive layers:

an outer Cr layer and an inter-diffusion zone (zone-1) underneath. Total thickness of the coating was approximately 45 μm. The EDS analysis (point 3) revealed that the inter-diffusion zone consisted of Cr and Ni. To accurately determine the phase composition of the multilayer structure coating inside, the micro-region XRD was determined and is shown in Fig. 1c. It can be observed that the Cr_2Ni_3 phase is the main constituent of the inter-diffusion zone according to the micro-region XRD pattern in Fig. 1c. Similarly, acicular Ti-rich phase was also present in the inter-diffusion zone of #2 coating.

Coatings with an Al content of 1.5 wt.%, 4 wt.%, 6 wt.% and 8 wt.% were co-deposited coatings of three-layer structures. Fig. 1d is the SEM cross-sectional image of coating #3, which consisted of three layers with a total thickness of approximately 80 μm: an outer Cr layer (1); an inner layer (2); an inter-diffusion zone with the columnar Cr layer (3) between the inner layer and substrate. From the EDS result of point 4 in layer 2 shown in Fig. 1f and micro-region XRD pattern from inner layer (zone-2) in Fig. 1d, it is evident that the major phases of the inner layer are NiAl and Ni_3Al. Elemental Cr (point 5) also exists.

The coatings with an Al content of 10 wt.% and 12 wt.% were aluminized coatings. Coating #4 is composed mainly of NiAl with a small amount of Cr and $AlCr_2$ (point 6); the thickness was 150 μm, as shown in Fig. 1e. Fig. 2 presents the concentration profiles of coating #3. As Fig. 2a shows, the coating can be clearly divided into three layers. A high Cr content was present in layer 2, indicating that the Cr has significant solubility in NiAl and Ni_3Al. Fig. 2b shows that enrichment of Co, Ti and Mo from the substrate appear mainly in the inter-diffusion zone of coating #3.

3.2 Oxidation resistance of coatings at 950℃ in air

Oxidation kinetics of coatings #1, #2, #3, and #4 after 100 h oxidation are drawn in Fig. 3. It is evident that coating #3 had much higher mass gains than the others. It suggests that the oxidation resistance of coatings #1, #2, and #4 was better than that of coating #3. Compared with the mass change of coatings #1, #2, and #4, the results further indicate that the oxidation resistance of coatings #1 and #2 is slightly better than coating #4 at 950℃ after 20 h. Fig. 4 presents the X-ray diffractograms of the coatings after oxidation at 950℃ for 100 h. According to Fig. 4, the phase constituents of coating #1 are Cr_2Ni_3 and Al_2O_3, chromized coating #2 consists of Cr_2O_3. Cr_2NiO_4, Al_2O_3 and NiO formed in the Al and Cr co-deposition coating #3. The oxide scale of coating #4 is mainly Al_2O_3.

Figs. 5a-h show the surface morphologies, cross-sectional images and EDS results of some areas in the coatings after oxidation at 950℃ for 100 h in air. Based on the EDS results in Fig. 5i, the agglomerate phase (point 1) in Fig. 5a is Al_2O_3. There is a substantial amount of Al_2O_3 oxide scale in the surface of coating #1 in Fig. 5b. Below the oxide layer, a large number of voids were generated in the unoxidized coating. The EDS results in Fig. 5i indicate that the oxide layers are made up of Cr_2O_3 (point 2) in Figs. 5c and d in coating #2. Compared with coating #1, the dominant phases of coating #2 are Cr and Cr_2Ni_3, and fewer voids exist in the Cr layer. A dense scale, consisting of Al_2O_3 (point 3), Cr_2NiO_4 (point 4), and NiO (point 5), was formed on

the surface of coating #3 as shown in Figs. 5e-f. The major oxide is Al_2O_3 (point 6) in the oxide layer. Below the oxide layer is NiAl, Ni_3Al (point 7), and Cr (point 8). Figs. 5g-h show that a continuous oxide Al_2O_3 (point 9) was formed on the surface of the #4 coating. Among the four types of coatings, the nearly 30 μm thick oxide layer of coating #3 was the thickest, which also reflects the results of Fig. 3.

4. Discussion

4.1 The formation of coatings

According to the comparison of four Al and Cr co-deposited coatings, it can be concluded that an increase of the Al content in the pack powder causes more aluminized coatings to emerge. When the pack's Al content is less than 1.2 wt.%, the coatings #1 and #2 consisted mainly of Cr and Cr_2Ni_3 with some Al-rich phase in coating #1. Coatings #1 and #2 show different features, and they are two types of chromized coatings. There exists Al-rich phase in coating #1, but this absent in coating #2. In short, when the Al content was more than 1.2 wt.% in the packs, chromized coating formed. Al and Cr co-deposited coating #3 can be formed simultaneously with the increase of the Al content in the packs. Elemental Cr and Al exist respectively in the form of Cr phase and NiAl + Ni_3Al phase presented in coating #3's multilayer structure. As the Al content increased to 10 wt.% in the packs, only aluminized coating exists. In the #4 aluminized coating, the Cr appeared in the form of $AlCr_2$.

Xiang et al. [14] analyzed the formation process of Al and Cr co-deposited coatings. In the initial stage, Al was deposited, and the aluminized coating layer NiAl and Ni_3Al was formed via inward diffusion of Al. Then, as the activity of Al decreased and the activity of Cr increased, the chromized material is more likely to react than the aluminized. However, the inter-diffusion zone mainly consisted of Cr. It confirmed that chromizing formed first, with the outward diffusion of Cr forming columnar Cr phase. When the chromizing is in process, the Cr diffuses from the substrate into the Cr layer, and then produces the inner NiAl and Ni_3Al layer and the outer Cr layer. The formation of coating #4 is mainly aluminizing. During the later stage, a large amount of Cr results in the formation of $AlCr_2$. Formulas for the chromizing reactions are shown below:

$$NH_4Cl\ (s) \rightarrow NH_3\ (g) + HCl\ (g) \quad (1)$$

$$2HCl\ (g) + Cr \rightarrow CrCl_2\ (g) + H_2\ (g) \quad (2)$$

$$3CrCl_2\ (g) \rightarrow [Cr] + 2CrCl_3\ (g) \quad (3)$$

$$2[Cr] + 3Ni \rightarrow Cr_2Ni_3 \quad (4)$$

As Fig. 1d and Fig. 2b show, some elements such as Co, Ti, and Mo diffused outward from the substrate to the inter-diffusion zone, with these chemical reactions occurring. In the chromized coating #2, Cr_2Ni_3 phase was present in the inter-diffusion zone; however, Cr_2Ni_3 phase had not formed in the Al and Cr co-deposition coating #3, instead, an inter-diffusion zone and an outer layer of Cr phase are present. This can be explained by a Ni selective reaction with Cr or Al, because Ni combined with Al from the substrate through the inter-diffusion zone, and Cr, Mo, Ti and other elements in

the substrate that moved by outward diffusion. Then the columnar Cr phase formed by outward-growth in the inter-diffusion zone. Compared with coating #3's columnar Cr layer (3), the morphology of the outer Cr layer (1) is not columnar. This illustrates that the outer Cr formed by chromizing deposition.

4.2 The mechanism of coatings oxidation resistance

Fig. 3 shows the weight gain of coating #3 was the largest. This can be explained from the coating microstructure. Firstly, the outer Cr layer was oxidized and formed a protective Cr_2O_3 scale. Then, because the outer Cr layer was thiner than other coatings (about 20 μm), the O_2 diffused into the next layer NiAl and Ni_3Al. Because of the formation of numerous NiO and Cr_2O_3, the Cr_2NiO_4 (Fig. 4, coating #3) formed in this stage. The chemical reactions of this process can be written as follows:

$$4[Al] + 3O_2 \rightarrow 2Al_2O_3 \quad (5)$$

$$2[Ni] + O_2 \rightarrow 2NiO \quad (6)$$

$$4[Cr] + 3O_2 \rightarrow 2Cr_2O_3 \quad (7)$$

$$Cr_2O_3 + NiO \rightarrow Cr_2NiO_4 \quad (8)$$

With the diffusion of O_2, large amounts of Al from the NiAl and Ni_3Al layer diffusing into the outer Cr layer led to the formation of Al_2O_3. Similarly with coating #3, the Al_2O_3 on the surface of coating #1 results from diffusion from the Al-rich phase. In part this is due to the Gibbs free energy of Al_2O_3 being more negative than that of Cr_2O_3 at 950℃. It is also worth noting that some studies [21, 22] have shown that the presence of Cr promotes the formation of Al_2O_3 scales on the coating surface, called the third element effect, which increases the thickness of the Al_2O_3 layer. These results indicated that the outer Cr layer has an important impact on the oxidation resistance of Cr and Al co-deposited coatings. Therefore, on the basis of the above analysis, Cr plays two roles in the process of coating oxidation. On the one hand, the formation of the harmful Cr_2NiO_4 phase cannot prevent the continuing oxidation of the coating. On the other hand, the presence of Cr in the NiAl and Ni_3Al layer promotes more Al_2O_3 generation than one sees in the NiAl coating #4. Compared with coatings#1 and #4, their oxide scales are Al_2O_3. However, some voids were formed near the oxide layer. Based on the research of Liu et al. [23], the thermal-expansion values of metals and oxides are different, and the compressive stresses in the oxide scales that causes scale spallation. Therefore, the compressive stresses between coating and oxide scale are also different. Obviously, the Al_2O_3 and NiAl coating are better matched in this regard than the Cr + Cr_2Ni_3 coating.

5. Conclusions

Co-deposition coatings of Al and Cr have been successfully prepared by one-step pack cementation. When the Al content is less than 1.2 wt.% in the pack powder, a chromized coating formed. With increasing Al content in the pack powder, Al + Cr co-deposited coatings of three-layer structure emerged. As the Al content increased further to 10 wt.% in the packs, only aluminized coating was present. The results of oxidation tests showed that the single aluminized and chromized coatings had better oxidation resistance than the co-deposited coatings of Al and Cr after oxidation at 950℃. Their oxide scales mainly consist of Al_2O_3 and Cr_2O_3, respectively. Higher Cr

contents in the Al + Cr co-deposited coatings stimulate the formation of Al_2O_3.

Acknowledgements

This work was supported by the National Natural Science Foundation of China (NSFC) under Grant 51271107, and the Shanghai Committee of Science and Technology, China under Grant No. 16520721700.

References

[1] T.M. Pollock, S. Tin, J. Propul. Power 22 (2006) 361.
[2] D.R. Clarke, C.G. Levi, Annu. Rev. Mater. Res. 33 (2003) 383.
[3] B. Gleeson, J. Propul. Power 22 (2006) 375.
[4] N.P. Padture, M. Gell, E.H. Jordan, Science 296 (2002) 280.
[5] G. N. Angelopoulos, N. Voudouris, N. Maragoudakis, J.K. Kiplagat, D. Tsipas, Mater. Manue. Process. 15 (2000) 605.
[6] Z.D. Xiang, J.S. Burnell-Gray, P.K. Datta, Surf. Eng. 17 (2001) 287.
[7] A.R. Castle, D.R. Gabe, Int. Mater. Rev. 44 (1999) 37.
[8] S. Rastegari, H. Arabi, M.R. Aboutalebi, A. Eslami, Can. Metall. Quart. 47 (2008) 223.
[9] X. Ledoux, M. Vilasi, S. Mathieu, P.J. Panteix, P. Del-Gallo, M. Wagner, Adv. Mater. Res. 278 (2011) 491.
[10] J. Kipkemoi, D. Tsipas, J. Mater. Sci. 31 (1996) 6247.
[11] M. Zheng, R.A. Rapp, Oxid. Met. 49 (1998) 19.
[12] P. A. Choquet, E. R. Naylor, R.A. Rapp, Mater. Sci. Eng. A 121 (1989) 413.
[13] W. Zhou, Y.G. Zhao, Q.D. Qin, W. Li, B. Xu, Mater. Sci. Eng. A 430 (2006) 254.
[14] Z.D. Xiang, S. R. Rose, P.K. Datta, Mater. Sci. Technol. 18 (2002) 1479.
[15] C. Zhou, H. Xu, S. Gong, Y. Yang, K.Y. Kim, Surf. Coat. Technol. 132 (2000) 117.
[16] Z.Y. He, Z.X. Wang, F. Zhang, Z.Y. Wang, X.P. Liu, Surf. Coat. Technol. 228 (2013) S287.
[17] S.C. Kung, R.A. Rapp, Oxid. Met. 32 (1989) 89.
[18] W.D. Costa, B. Gleeson, D.J. Young, J. Electrochem. Soc. 141 (1994) 1464.
[19] H.L. Du, J. Kipkemoi, D.N. Tsipas, P.K. Datta, Surf. Coat. Technol. 86-87 (1996) 1.
[20] B. Gleeson, W.H. Cheung, W.D. Costa, D.J. Young, Oxid. Met. 38 (1992) 407.
[21] Z.G. Zhang, F. Gesmundo, P.Y. Hou, Y. Niu, Corros. Sci. 48 (2006) 741.
[22] F.H. Stott, G.C. Wood, J. Stringer, Oxid. Met. 44 (1995) 113.
[23] Z. Liu, W. Gao, K.L. Dahm, F. Wang, Oxid. Met. 50 (1998) 51.

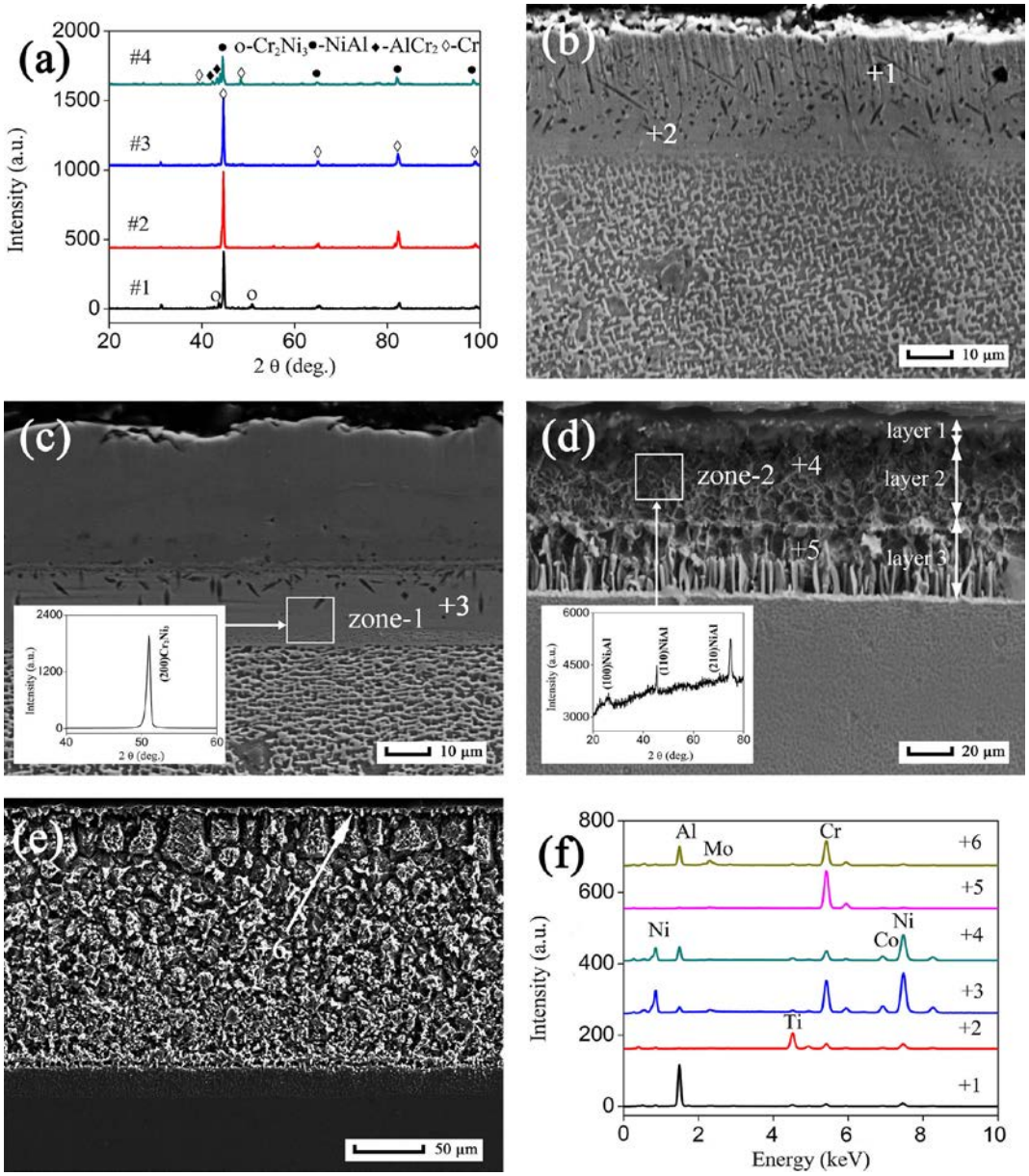

Fig. 1. X-ray diffractograms (a), SEM cross-sectional images of coatings (b) #1, (c) #2, (d) #3, and (e) #4, and (f) EDS results of different phases in coatings.

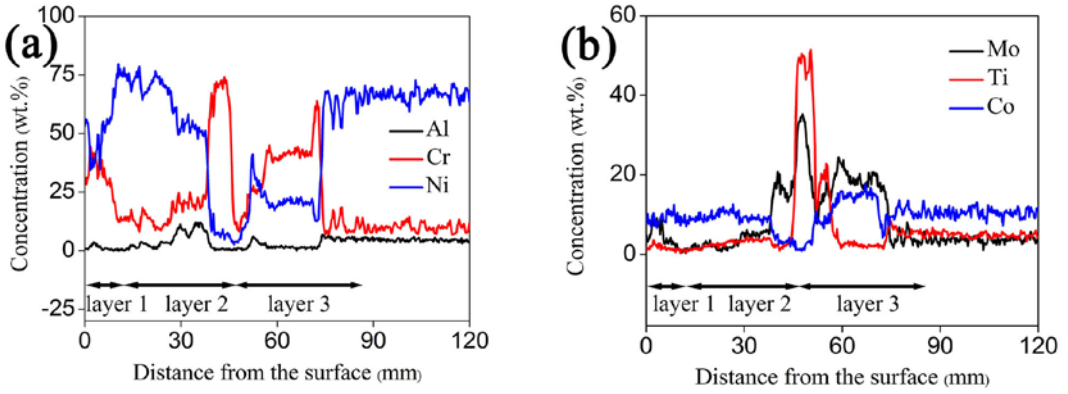

Fig. 2. Concentration profiles of the elements (a) Al, Cr, Ni, (b) Ti, Mo, and Co in coating #3.

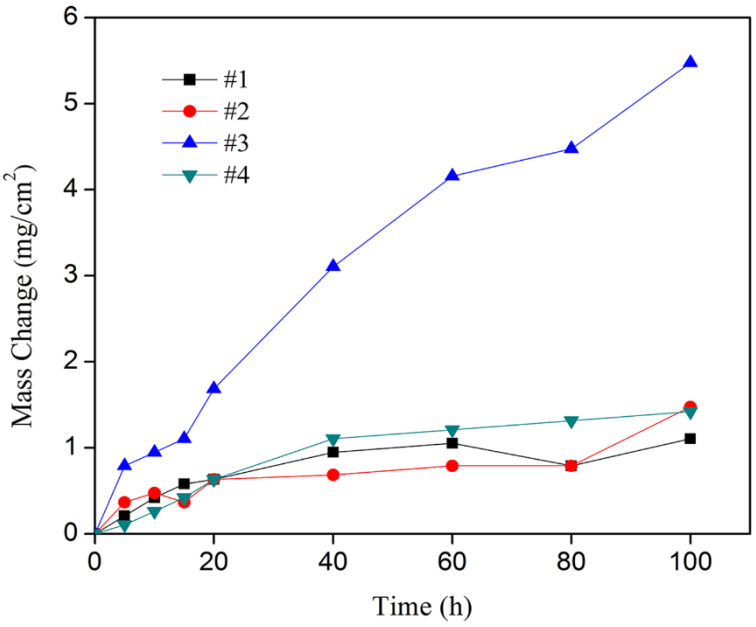

Fig. 3. Isothermal oxidation kinetics of the coatings after oxidation at 950℃ in air.

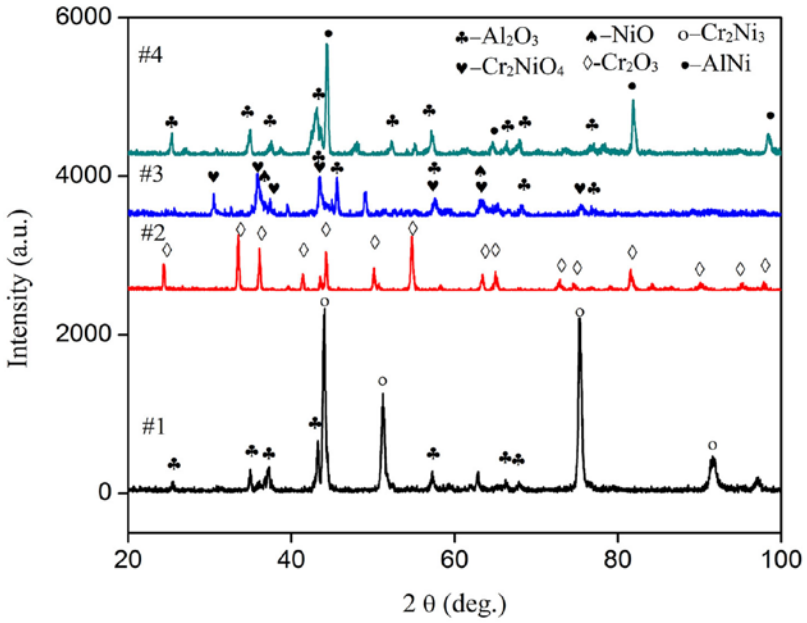

Fig. 4. X-ray diffractograms of the coatings after 100 h oxidation at 950℃ in air.

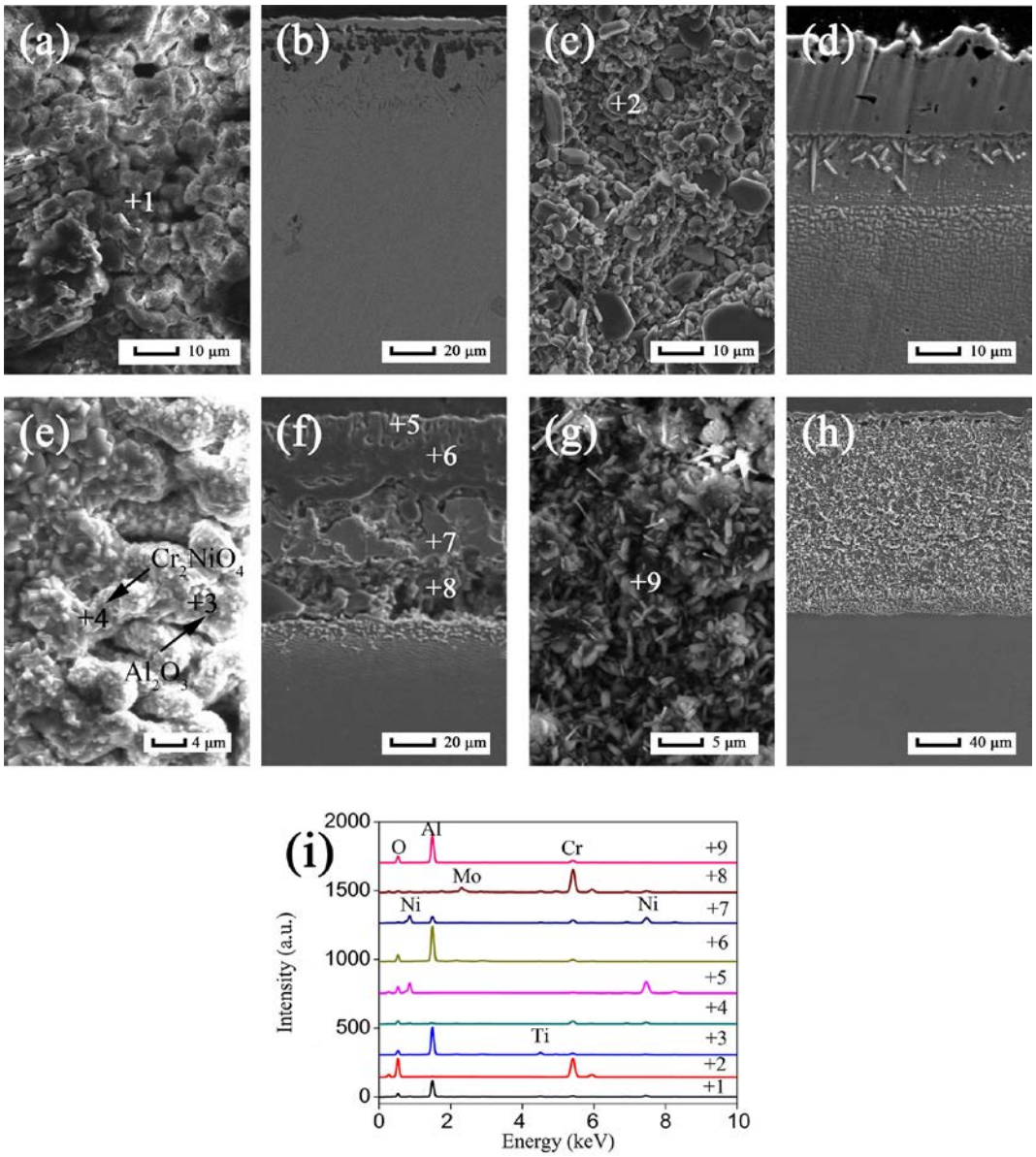

Fig. 5. (a), (c), (e), and (g) SEM images of surface morphologies; (b), (d), (f), and (h) SEM images of cross sections of the #1, #2, #3, and #4 coatings after 100 h oxidation at 950℃ in air, and (i) EDS results of different phases in coatings.